

PHYSICS OF MAGNETIC PHENOMENA

INFLUENCE OF RADIATION-THERMAL TREATMENT ON THE PHASE COMPOSITION AND STRUCTURAL PARAMETERS OF THE SHS PRODUCT BASED ON W-TYPE HEXAFERRITE

E. P. Naiden,¹ R. V. Minin,² V. I. Itin,² and V. A. Zhuravlev¹

UDC 538.62; 548:537.611.46

The phase composition, structural parameters, and main magnetic characteristics of BaCo_{0.7}Zn_{1.3}Fe₁₆O₂₇ hexaferrites obtained by the method of self-propagation high-temperature synthesis in combination with mechanochemical activation and radiation-thermal post-sintering are investigated. It is established that the suggested method is promising for synthesis of ferrite ceramics with hexagonal composition and optimal magnetic properties.

Keywords: SHS, hexaferrites, ferromagnetic resonance, magnetocrystalline anisotropy, radiation-thermal synthesis, mechanical activation.

INTRODUCTION

Oxide ferromagnetic materials (ferrites) are widely used in various fields of modern technology and medicine. Industrial production of ferrites and their products is based on the conventional multi-operational ceramic technology which involves a number of long-running operations. This technology has been used in the world practice for many decades, and its development is associated with optimization by adjusting the charge composition and treatment method. Thus, for example, sintering of ferrites in vertical furnaces under dynamic conditions of phase formation with granulated charge allows the productivity of the process of ferrite powder synthesis to be sharply increased retaining the high level of ferrite properties [1].

In the last decades, new methods of ferrite synthesis have been proposed based on self-propagating high-temperature synthesis (SHS) in the regime of filtration combustion of the mixture of powders comprising iron and oxide of some elements in the atmosphere of reacting gases: oxygen or air [2]. This method utilizes the internal chemical energy of the initial reagents, and is organized most favorably from the thermal viewpoint. In the process of obtaining ferrites, it substitutes the most important operation – ferritization – which in the conventional method of sintering is very long and proceeds at high temperatures.

The SHS method allows various cubic ferrites and hexagonal ferrites with M-phase composition to be synthesized. However, the yield of the end product of synthesis of complex hexagonal barium and strontium ferrites with W-, Y-, and Z-compositions is low. In this regard, new resource-saving methods of synthesis of magnetic materials based on complex hexaferrites with W-composition are suggested with the SHS, mechanochemical pre- or post-activation, and final ferritization in electric furnaces [3, 4] that in comparison with the conventional methods allow the energy and material expenses for the production process to be reduced significantly. It is of interest to substitute the final ferritization operation in an electric furnace by radiation-thermal sintering (RTS) upon exposure to an electron

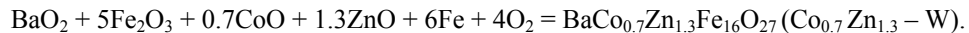
¹National Research Tomsk State University, Tomsk, Russia; ²Department of Structural Macrokinetics of the Siberian Branch of the Russian Academy of Sciences, Tomsk, Russia, e-mail: ptica@mail.tsu.ru. Translated from *Izvestiya Vysshikh Uchebnykh Zavedenii, Fizika*, No. 6, pp. 63–68, June, 2013. Original article submitted April 11, 2013.

beam. This process sharply accelerates ion diffusion due to joint thermal and radiation influence on the material and as a result, improves the magnetic properties of the synthesized materials [5].

The present work is aimed at investigation of the influence of radiation-thermal sintering on the phase composition, structural parameters, and magnetic properties of the multiphase product based on barium hexaferrite with W-composition obtained by the method of self-propagating high-temperature synthesis.

EXPERIMENTAL AND RESULTS

To synthesize barium hexaferrite with W-composition, we used the chemical reaction



Barium hexaferrite with W-type composition was synthesized in following regimes:

- **No. 1:** SHS,
- **No. 2:** SHS with mechanical activation of the initial charge for 3 min for the grinding body mass to the powder mass in the ratio 20:1 that corresponded to a milling process power of 60g (MA3+SHS),
- **No. 3:** SHS with mechanical post-activation of the product for 40 min for the grinding body mass to the powder mass in the ratio 10:1 that corresponded to a milling process power of 40g (SHS+MA40).

Mechanical activation (MA) was carried out in the air atmosphere in an MPV planetary mixing mill with water cooling, the steel cylinder volume was 1000 cm³, and balls made of ball-bearing steel (1.5% Cr) ~5 mm in diameter were used for grinding.

Tablets were pressed from the product obtained by single-ended cold pressing at room temperature in a PGr-10 hydraulic press. A 10% solution of polyvinyl alcohol was used as a softener. Weighed 2.5 g samples were loaded into a cylindrical compression mould 20 mm in diameter and pressed under pressure of 35–40 MPa for 5 min.

Radiation-thermal sintering of samples was carried out at the Institute of Nuclear Physics of the Siberian Branch of the Russian Academy of Sciences (Novosibirsk) using an ILU-6 pulsed electron accelerator [6]. The electron energy was 2.4 MeV, the beam current per pulse was 400 mA, the pulse duration was 500 µs, and the pulse repetition frequency was 7–15 Hz. The average radiation power in the regime of isothermal annealing was ~3 kGy/s. The dose power per pulse was 800 kGy/s. Samples were irradiated in a special heat-insulating box made of lightweight fireclay. Nonisothermal stages of annealing (heating and cooling) lasted ~3 min.

After heating of the product to a preset temperature of 1050–1250°C, the radiation pulse repetition frequency was adjusted so that to stabilize the temperature. The sample was held in this regime for 120 min. Then the pulse repetition frequency was reduced so that the rate of sample cooling was ~20 deg/min. In this regime, the ferrite temperature decreased to 350–400°C; then the accelerator was switched off and the product was cooled spontaneously to room temperature.

The x-ray analysis was performed using a SHIMADZU XRD-6000 polycrystal diffractometer. X-ray diffraction patterns were registered in the Bragg–Brentano geometry with a focusing shaped pyrographite crystal-monochromator inserted into the second beam of gamma quanta.

For a qualitative analysis of the phase composition, the computer database of x-ray powder diffractometry or PDF4+ of the International Center of Diffraction Data (ICDD, Denver, USA) was used. The quantitative analysis of the phase composition and the refinement of the structural parameters of phases being detected were performed using the program *Powder Cell 2.4* for full profile analysis.

Results of x-ray structural analysis of ferrite ceramic samples after RTS are presented in Table 1.

From Table 1 it follows that the yield of the target (W) phase at RTS temperatures of 1200–1250°C is about 90–98 vol.%; moreover, sufficiently high internal elastic microstresses remain for all compositions. The mean microcrystallite size increases with RTS temperature.

The morphological characteristics of hexagonal ferrimagnetic materials synthesized by a combination of SHS and RTS methods were analyzed using a Philips 515 electron microscope with different magnifications. Results of the scanning microscopy for some samples are shown in Fig. 1.

TABLE 1. Influence of RTS Regimes of the SHS Product on the Phase Composition and Structural Parameters of Barium Hexaferrite

Sample	Phase composition of the product, vol. %			Mean W-phase crystallite size, nm	$\Delta d/d \cdot 10^3$
	W-phase	Fe_3O_4	Fe_2O_3		
No. 1 + RTS at 1050°C	45	50	5	67	0.6
No. 1 + RTS at 1100°C	54	40	6	46	1.3
No. 1 + RTS at 1200°C	93	7	—	170	1.9
No. 1 + RTS at 1250°C	98.4	1.4	0.2	>500	0.2
No. 2 + RTS at 1050°C	39	54	6	100	0.9
No. 2 + RTS at 1100°C	53	46	1	140	0.7
No. 2 + RTS at 1200°C	89	11	—	>300	0.2
No. 2 + RTS at 1250°C	54	40	6	400	0.2
No. 3 + RTS at 1050°C	64	28	8	110	0.3
No. 3 + RTS at 1100°C	53	41	6	135	0.7
No. 3 + RTS at 1200°C	88	12	0	140	0.4
No. 3 + RTS at 1250°C	93	7	—	>300	0.2

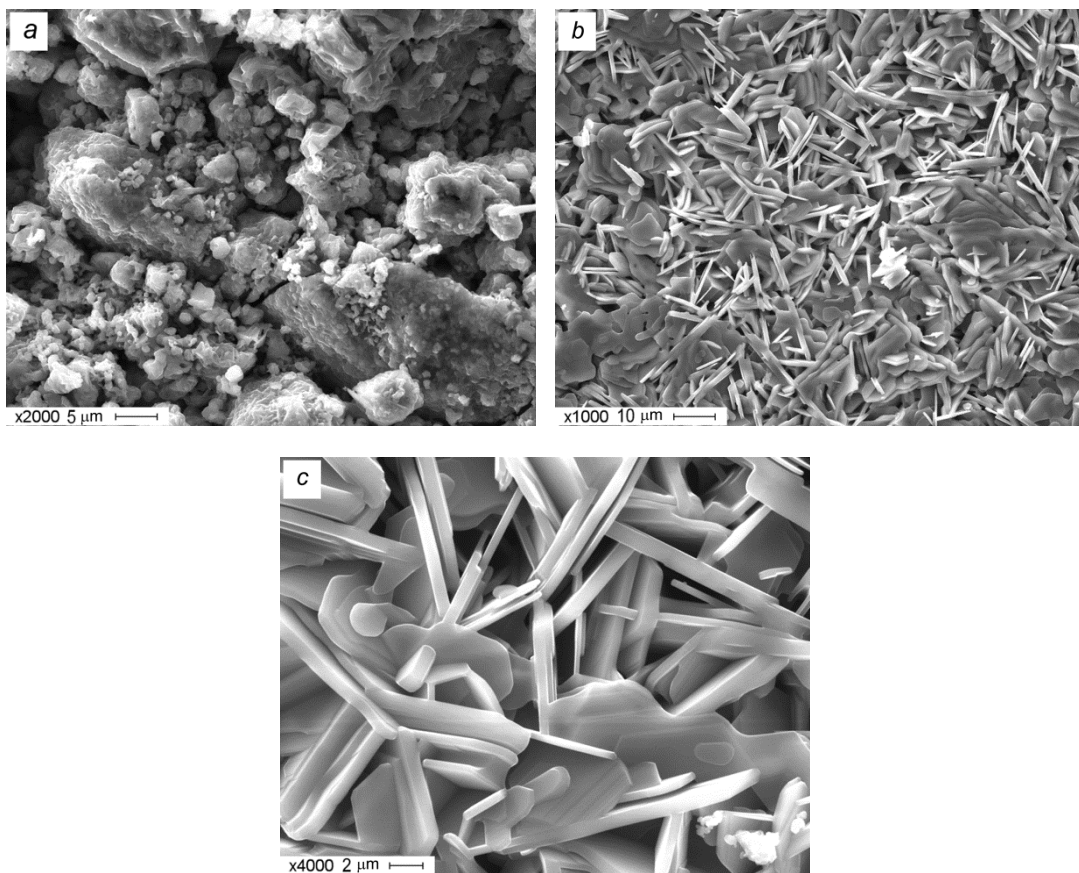


Fig. 1. Scanning microscopy: a) No. 1 + RTS at 1100°C; b) and c) No. 1 + RTS at 1250°C with indicated magnifications.

The morphology of samples obtained at RTS temperatures of 1100–1200°C was characterized by the presence of grains having quasi-spherical shapes characteristic for cubic ferrospinel along with particles shaped as hexagonal

TABLE 2. Results of Static Measurements of the Magnetic Parameters of Samples

Sample	M_S , G	$H_{a\text{ eff}}$, kOe
No. 1 + RTS at 1200°C	493	2.03
No. 2 + RTS at 1200°C	487	2.23
No. 3 + RTS at 1200°C	482	2.41
No. 1 + RTS at 1250°C	484	2.22
No. 2 + RTS at 1250°C	487	2.43
No. 3 + RTS at 1250°C	447	1.89

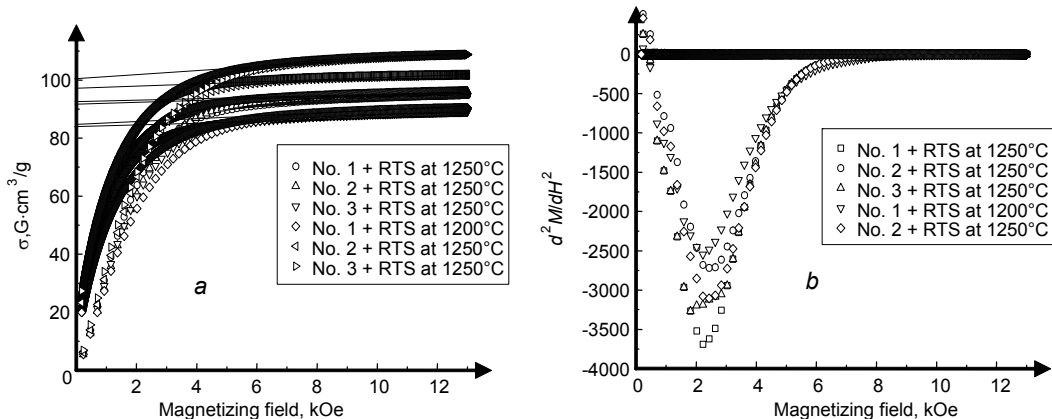


Fig. 2. Magnetization curves (a) and their second derivatives (b) for the indicated examined samples.

plates whose linear size and thickness were in the aspect ratio $a/c \approx 10$ typical for ferrites with hexagonal composition. An increase in the RTS temperature to 1250°C caused a significant change of the morphology of ferrite ceramics with hexagonal composition. Quasi-spherical particles practically disappeared, and the aspect ratio a/c of hexaferrite crystallites considerably increased (to ≈ 20).

The static magnetic characteristics of ferrite ceramic samples, including the specific saturation magnetization and effective magnetic anisotropy field, were investigated using an automated plant intended for investigation of the magnetic characteristics in pulsed magnetic fields. The measurement procedure was described in detail in [7].

Figure 2 shows the magnetization curves (Fig. 2a) and their second derivatives (Fig. 2b) for samples with maximum content of the $\text{Co}_{0.7}\text{Zn}_{1.3}$ -W target phase. Linear extrapolation of high-field sections of the magnetization curves toward zero magnetizing fields yields the specific saturation magnetization (σ). The magnetizing fields corresponding to minima of the second derivatives provide estimates of the effective anisotropy fields ($H_{a\text{ eff}}$).

The main magnetic characteristics: the saturation magnetization $M_S = \sigma \cdot \rho$ (ρ is the x-ray density of samples) and the effective anisotropy fields for samples with maximum content of the $\text{Co}_{0.7}\text{Zn}_{1.3}$ -W target phase are presented in Table 2.

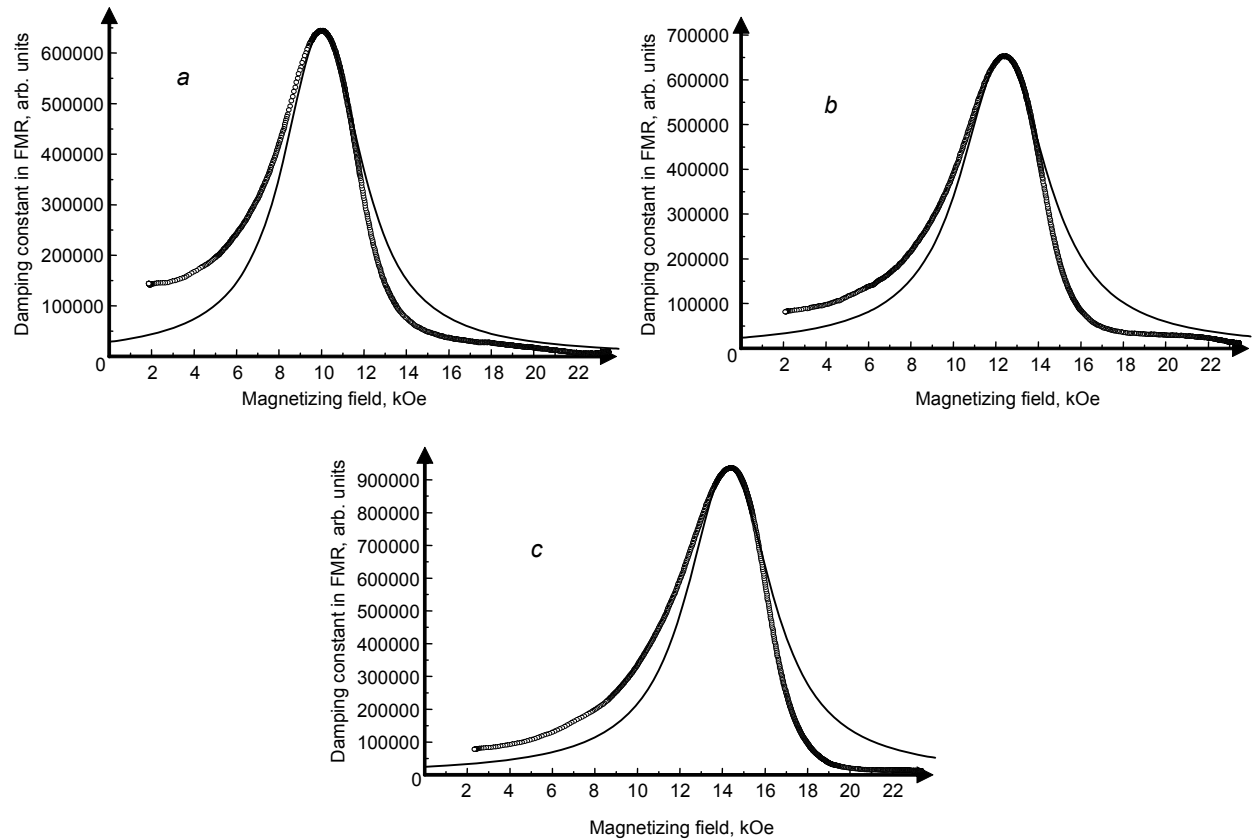
Investigations of the ferromagnetic resonance spectra of powder and polycrystalline oxide ferrimagnetic materials with hexagonal crystal composition allowed a number of magnetic parameters of these materials important for practical applications to be determined [8], including

- magnitude and sign of magnetocrystalline anisotropy fields (H_{ai});
- value of the magnetomechanic ratio $\gamma = ge/2mc$, where g is the g-factor of the examined material, e is the electron charge, m is the electron mass, and c is the velocity of light;
- saturation magnetization (M_S).

The ferromagnetic resonance (FMR) spectra were measured by the standard waveguide transmission technique in the frequency range 26–37 GHz using an automated radio spectroscope built around a P2-65 analog scalar circuit analyzer. To investigate the FMR, hexaferrite powders were loaded into quartz tubes with inner diameter of 0.7 mm and

TABLE 3. Damping Constants of Calculated Curves

Sample	α , 26 GHz	α , 32 GHz	α , 37 GHz
No. 1 + RTS at 1200°C	0.2	0.18	0.16
No. 2 + RTS at 1200°C	0.13	0.12	0.11
No. 3 + RTS at 1200°C	0.12	0.11	0.10
No. 1 + RTS at 1250°C	0.21	0.18	0.16
No. 2 + RTS at 1250°C	0.17	0.15	0.13
No. 3 + RTS at 1250°C	0.14	0.12	0.10


 Fig. 3. FMR spectra of sample No. 1 + RTS at 1250°C: a) $f = 26$ GHz, b) $f = 32$ GHz, and c) $f = 37$ GHz.

length of 10 mm. The density of powder samples was identical and equal to ≈ 2.9 g/cm³. The spectra were processed using the procedure described in [8, 9].

Figure 3 shows the FMR spectra calculated in the approximation of independent grains (solid curves) together with the experimental FMR spectra (open circles) for sample No. 1 + RTS at 1250°C at three frequencies from the examined range. The measurement frequencies are indicated in the figure caption.

The frequency dependences of the Gilbert damping constant (α) in the Landau–Lifshits equation of motion for individual single crystal grain are tabulated in Table 3. The given parameter depends in a complicated manner on the morphological and magnetic characteristics of crystallites in the material and on the experimental conditions. According to Table 1, the frequency increase for all investigated samples caused the damping constant to decrease due to the ordering effect of the applied magnetic field, because the field in resonance increased with frequency.

Any inhomogeneities caused either by the spread of the crystallite shapes or anisotropy fields over the sample grains in the examined material result in the increased parameter α . From the data presented in Table 1 it follows that

TABLE 4. Magnetic Parameters of Materials Measured by the FMR Method

Sample	$\gamma/2\pi$, GHz/kOe	H_{al} , kOe	M_s , G
No. 1 + RTS at 1200°C	2.56	-0.8	440
No. 2 + RTS at 1200°C	2.62	-1.5	520
No. 3 + RTS at 1200°C	2.62	-1.5	525
No. 1 + RTS at 1250°C	2.58	-1.0	490
No. 2 + RTS at 1250°C	2.58	-1.0	480
No. 3 + RTS at 1250°C	2.58	-1.0	450

samples without mechanical activation (No. 1 + RTS at 1200°C and No. 1 + RTS at 1250°C) have much greater damping constants than mechanically activated samples. This demonstrates a higher degree of inhomogeneity of the materials. Moreover, the increase of the mechanical activation time from 3 to 40 min leads to the decrease in α which corresponds to the increased degree of homogeneity of the samples.

The increase of the RTS temperature from 1200 to 1250°C leads to an insignificant increase in the damping constant. Thus, the mechanical activation promotes the increased homogeneity of the samples obtained and the decrease of the RTS temperature.

Table 4 presents the magnetomechanic ratios, anisotropy fields, and saturation magnetizations of the synthesized materials. The parameters $\gamma/2\pi$ and H_{al} were estimated from a comparison of the positions of maxima for theoretical and experimental curves of ferromagnetic resonance at different frequencies. The saturation magnetizations were determined according to the Standard of the Enterprise STO TGU 030-2009 from the measured resonant fields for two orientations of the cylindrical sample with respect to the magnetizing field.

Values of the saturation magnetization M_s given in Table 3 are close to M_s values estimated from the measured magnetization curves (see Table 2). The difference between M_s values measured by different methods did not exceed 10%. We note that the negative sign of the anisotropy field H_{al} demonstrates that the anisotropy of easy magnetization type is observed for these materials. The measured fields are close to those obtained from analysis of magnetization curves in pulsed fields and to the literature data for these materials synthesized by the conventional ceramic technology [9].

In the first series of samples (RTS at a temperature of 1200°C), the mechanical activation leads to an increase in $\gamma/2\pi$ and H_{al} values estimated from the FMR experiment. Processing of the data of experiments for samples of the second series demonstrated that $\gamma/2\pi$ and H_{al} values for these materials coincide within the limits of the experimental errors.

Thus, the technology combining SHS, mechanical activation, and radiation-thermal sintering allows complex multicomponent ferromagnetic materials to be synthesized with hexagonal crystal composition and magnetic characteristics no worse than and in some cases even higher than the corresponding characteristics of samples synthesized by the conventional ceramic technology. An advantage of the suggested technology is a significant decrease of the time of synthesis and energy consumption.

This work was supported in part by the Federal Target Program “Research and Development for Priority Directions of Development of Science and Technology Complex of Russia for 2007–2013” (State Contract No. 14.513.11.0055).

REFERENCES

1. L. M. Letyuk, G. Nauman, A. B. Gonchar, *et al.*, in: Materials of the 4th Russian-Japanese Seminar “Perspective Technologies and Equipment for Materials Science and Micro- and Nanoelectronics,” Part 2 [in Russian], Moscow; Astrakhan’ (2006), pp. 12–15.
2. A. G. Merzhanov and M. D. Nersesyan, Zh. Vsesoyuzn. Khim. Obshch. Imeni D. I. Mendeleeva, **35**, No. 6, 700–707 (1990).

3. R. V. Minin, Technology of synthesis of hexagonal oxide ferrimagnetic materials with W-, M-, and Z-compositions by the method of self-propagating high-temperature synthesis, Cand. Tech. Sci. Dissert., Tomsk Polytechnic University, Tomsk (2008).
4. V. I. Itin, A. I. Kirdyashkin, R. V. Minin, *et al.*, Izv. Vyssh. Uchebn. Zaved. Tsvetn. Metallurg., No. 5, 83–88 (2006).
5. V. I. Vereshchagin, P. M. Pletnev, A. P. Surzhikov, *et al.*, Functional Ceramics, V. I. Vereshchagin, ed. [in Russian], Publishing House of the Institute of Inorganic Chemistry of the Siberian Branch of the Russian Academy of Sciences, Novosibirsk (2004).
6. V. L. Auslender, A. A. Bryazgin, L. A. Voronin, *et al.*, Nauka – Proizv., No. 7, 11–17 (2003).
7. V. Yu. Kreslin and E. P. Naiden, Prib. Tekh. Eksp., No. 1, 63–68 (2002).
8. E. P. Naiden, V. I. Itin, R. V. Minin, *et al.*, Russ. Phys. J., **55**, No. 8, 869–877 (2012).
9. V. A. Zhuravlev, Fiz. Tverd. Tela, **41**, No. 6, 1050 (1999).